Chapter 7

Epitaxial Growth of Mn on Si(111)

7.1 Introduction

There are a few reports and experiments concerning the adsoption of Mn on Si(111), where film growth with and without a Bi surfactant layer [18–21,156], surface structural phase transitions [157], as well as a non-metal-to-metal phase transition in 5-10 monolayers thick films [158] have been reported. Kumar *et al* observed with low-energy electron diffraction (LEED) that at low coverage silicide islands form which turn into a nearly closed film at higher coverage [22].
In the matter of morphology of Mn-silicide films, a Volmer-Weber-like growth mode is supposed in these reports.

7.2 Low Coverage Adsorption

There are a number of experimental and theoretical studies on the reconstructions of the bare Si(111) surface. It has been established that this surface has a (7×7) reconstruction of Takayanagi type[1] [117], which undergoes a phase transition to a high temperature phase, a (1×1) structure, at 870 °C. A host of other reconstructions of the clean Si(111) (9×9), (5×5), (2×2), $c(2 \times 4)$, and $(\sqrt{3} \times \sqrt{3})$ have been reported from scanning tunneling microscopy (STM) experiments [159].

Adsorption of Mn on Si(111) leads to the formation of a closed metallic film at a coverage of more than 5 ML and exhibiting a $(\sqrt{3} \times \sqrt{3})$ surface reconstruction [22].

The present calculations are performed in order to find the low coverage (for a coverage of 0.5 ML) adsorption site of Mn in the (1×1) surface unit cell. For simulating

---

[1]This model basically consists of 12 adatoms arranged locally in the (2×2) structure, nine dimers on the sides of the triangular subunits of the (7×7) unit cell and a stacking fault layer.

(top-side view) 1fold overlayer (O_1) (top-side view) 3fold chain (C_3)

(top-side view) 3fold hollow (H_3) (top-side view) 4fold atop (T_4)

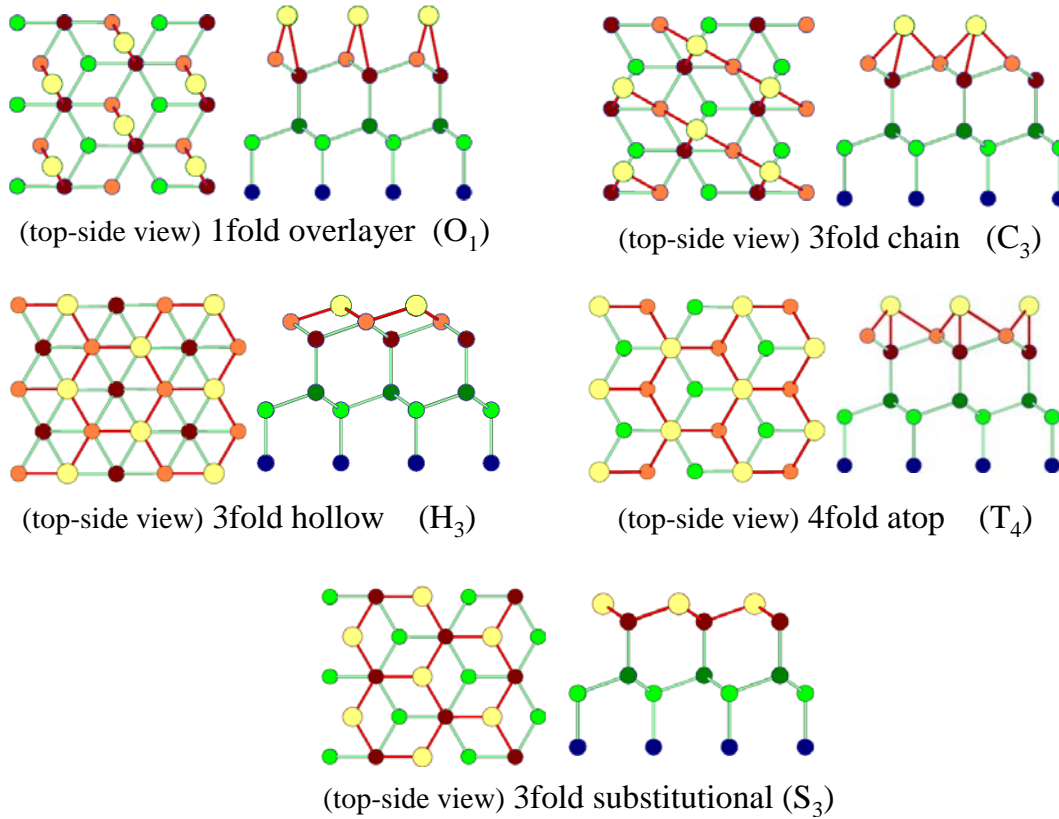(top-side view) 3fold substitutional (S_3)

Fig. 7.1: Top-view (left figure in each structure) and side-view (right figure in each structure) for five configurations of Mn adsorbed on the Si(111) surface. The big yellow circles represent Mn atoms, while all the small circles depict Si atoms in different layers. O_1 is an overlayer site with one-fold coordination to a surface atom. C_3 is a 3-fold mono-atomic chain and H_3 is the 3-fold hollow sites. T_4 is a 4-fold atop site and S_3 is a 3-fold substitutional site.

silicide films a $(\sqrt{3} \times \sqrt{3})$ unit cell is used. There are two kinds of common adsorption sites on the (111)-(1×1) surface of the diamond crystal structure.

One of them is a four-fold atop site, T_4, which was proposed by Northrup [160]. In this model the adatom has four Si neighbors, three in the surface layer and one in the second layer directly below. Adsorption in this position can eliminate the surface dangling bonds.

The second one is a three-fold hollow site, H_3, in which the adatom forms just 3 bonds with the surface layer atoms. Such an arrangement leads to the disappearance of surface dangling bonds, as well.

In 1964, Lander and Morrison suggested that the hollow site, H_3, is the most stable adsorption site for adsorption of a Si-adatom on Si(111) [161]. Later on, in 1989, Kohmoto *et al.* [162] showed, following the analysis of reflective high electron en-

ergy diffraction (RHEED) intensity at 900 °C, that Si-adatoms are adsorbed in both the T_4 and the H_3 sites with a mixing ratio of about 4:1. This means that the T_4 position is more stable than the H_3 site.

Besides these two known sites (i.e. T_4 and H_3), we also calculated the adsorption energy in other positions, such as the overlayer site (O_1), the mono-atomic-chain site (C_3) and the substitutional site (S_3), all shown in Fig. 7.1. The substitutional sites S_4 and S_6, see Fig. 7.2, were considered as well. We point out that adsorption of a single Mn in a (1×1) cell coresponds to a 0.5 ML coverage.

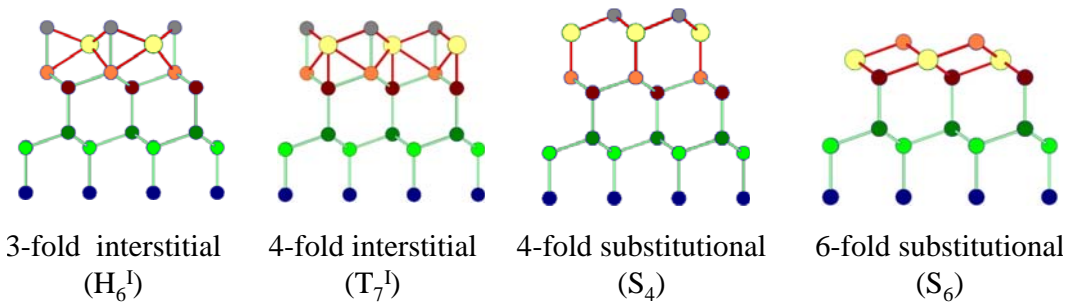| 3-fold interstitial (H_6^I) | 4-fold interstitial (T_7^I) | 4-fold substitutional (S_4) | 6-fold substitutional (S_6) |

Fig. 7.2: Side view of structures with hollow, atop and substitutional site adsorption and a Si-covering layer. In most of the structures, the surface dangling bonds are saturated and the Mn atoms below the surface are highly coordinated.

As it was discussed in chapter 4, the bare Si surface in (111) orientation can be either the single-dangling-bond (shuffle-terminated faces), SDB, or the triple-dangling-bond (glide-terminated faces), TDB structure. Since the TDB surface is less stable than the SDB surface[2], it is not surprising that the released energy due to the adsorption on the TDB surface becomes larger than on the SDB surface.

Fig. 7.1 shows the configurations for Mn adsorbed at the topmost layer of either SDB or TDB. There are four possible adsorption sites on the SDB surface, the O_1,C_3, H_3 and T_4 sites, while only one adsorption site, called S_3, is found on the TDB surface. Mn in a O_1 binds to the corner of surface triangles with only one bond, so that one surface dangling bond per cell still remains. The energy gain from the adsorption in this position is 2.557 eV [3]. An adatom in the C_3 configuration is three-fold coordinated to the substrate atoms and sits on the side of substrate triangles. Adatoms and surface atoms form alternating mono-atomic chains and surface dangling bonds are completely saturated. This configuration is more stable than O_1 site by 0.174 eV. For adsorption of Mn at the topmost layer on the SDB surface, the H_3 is found to be favored over the T_4 site by 0.184 eV; the energy gained from the H_3

---

[2]The surface energy, γ, is 1.303 and 2.279 eV/(1×1) cell for the SDB and TDB, respectively.

[3]In order to calculate the adsorption energy, the total energy of the bare Si(111) surface and the total energy of the free Mn atom are considered as reservoirs, see eq. 5.1 chap.4.

site adsorption is 3.248 eV. The S_3 structure corresponds to the adsorption of Mn at the TDB surface. The adatom is substituted in the place of the substrate atom. The adsorption energy is 4.130 eV but formation energy of this structure is less than H_3 structure.

Since it was concluded from adsorption on Mn on Si(001) that the presence of a Si-capping layer increases the stability of the system, the effect of a capping layer on the Si(111) surface will be studied by adding a Si layer on top of the Mn layer, Fig. 7.2. The subsurface six-fold hollow site, H_6^I, and the seven-fold atop site, T_7^I, are interstitial sites. They resemble the H_3 and T_4 sites, but have an overlayer of Si on top. The adsorption energies are 4.271 eV and 4.537 eV, calculated with respect to the TDB surface. Similarly to the results for the (001) surface, the additional Si capping layer increases the stability in both cases.

In both S_4 and S_6 substitutional structures, one Si atom from the SDB surface is replaced by a Mn atom. The Si-bulk is considered to be the reservoir for the replacement.
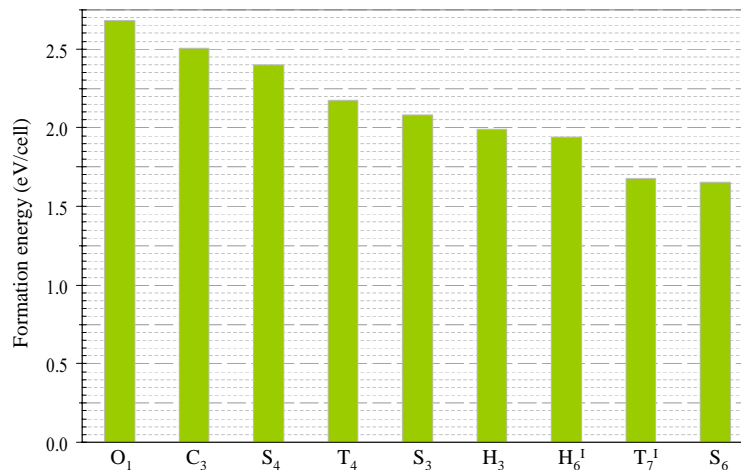

Fig. 7.3: Formation energy for all the considered structures in eV per (1×1) cell. The six-fold substitutional site, S_6 on the SDB surface with a Si capping layer is the most stable adsorption site for Mn on this surface.

The formation energies [4] for the different considered structures are listed in chart. 7.3. The lowest formation energy belongs to the position in which a single Mn atom sits in a six-fold substitutional site on the SDB surface with a Si-capping layer. The tendency of Mn atoms to penetrate into the subsurface region can be explained with an increased coordination of the adatoms and the formation of strong Mn-Si bonds.

The Si overlayer has also a considerable effect on the thermodynamic stability of

---

[4]For the calculation of the formation energy the total energy of the bulk phase of each constituent part is considered as a reservoir.

Table 7.1: The distance between Mn and Si in the first (Si_1) and the second (Si_2) substrate layer in Å , Mn magnetic moment and first layer Si magnetic moment (in μ_B) for different adsorption sites of Mn on Si(111).

site	Mn-Si_1 distance (Å)	Mn-Si_2 distance (Å)	Mn-spin moment (μ_B)	Si_1-spin moment (μ_B)
O_1	2.33	2.72	3.74	-0.04
C_3	2.45	2.62	3.60	-0.04
H_3	2.34	2.71	3.12	-0.02
T_4	2.58	2.34	3.51	-0.04
S_3	2.38	—	3.44	-0.15
H_6^I	2.45	2.66	3.24	-0.09
T_7^I	2.42	2.68	2.20	-0.14
S_4	2.29	2.38	2.45	-0.24
S_6	2.37	2.39	2.56	-0.04

the atop positions (T_4). The capping layer increases the stability of this position (i.e. T_7^I site) by almost 0.50 eV relative to the T_4 site, while the energy difference between H_3 and H_6^I is just 0.05 eV.

The magnetic moment of Mn induces a small magnetic moment in opposite direction in the substrate atoms in these structures. The bonds lengths of Mn with the Si atoms of the first (Si_1) and second (Si_2) substrate layers, as well as the magnetic moments of the Mn and the Si_1 atoms are presented in the Tab. 7.1. The magnetic moment of the Si layer closest to the Mn layer has antiparallel coupling to the latter. The presence of a Si overlayer leads to a significant reduction of the magnetic moment of Mn, which is due to a large overlap between the Mn and Si orbitals, see Fig. 7.4. The DOS plot of configurations with a Si-overlayer, i.e. S_6, H_6^I and T_7^I (Mn-overlayer, i.e. S_3, H_3 and T_4) for the majority and the minority spin channel are shown on the left side (right side) plot of Fig. 7.4.

In DOS of the T_4 configuration, there is a sharp peak around -3.5 eV, while due to the stronger overlap between Mn-d and Si-sp orbitals in the T_7^I position, the band width is broader compared to the T_4 structures. Furthermore, the Si-capping layer shifts some electrons in minority spin states of the T_7^I structure to lower energy, below the Fermi level and also decreases the occupation number of states at the Fermi level. This results in the T_7^I configuration becoming more favorable than the T_4 structure. Aditionally, the presence of the Si-capping layer in the T_7^I structure shifts the position of the Fermi level of T_4 by +0.22 eV. This causes an increase of filled state in the minority spin channel which reduces magnetic moment and de-

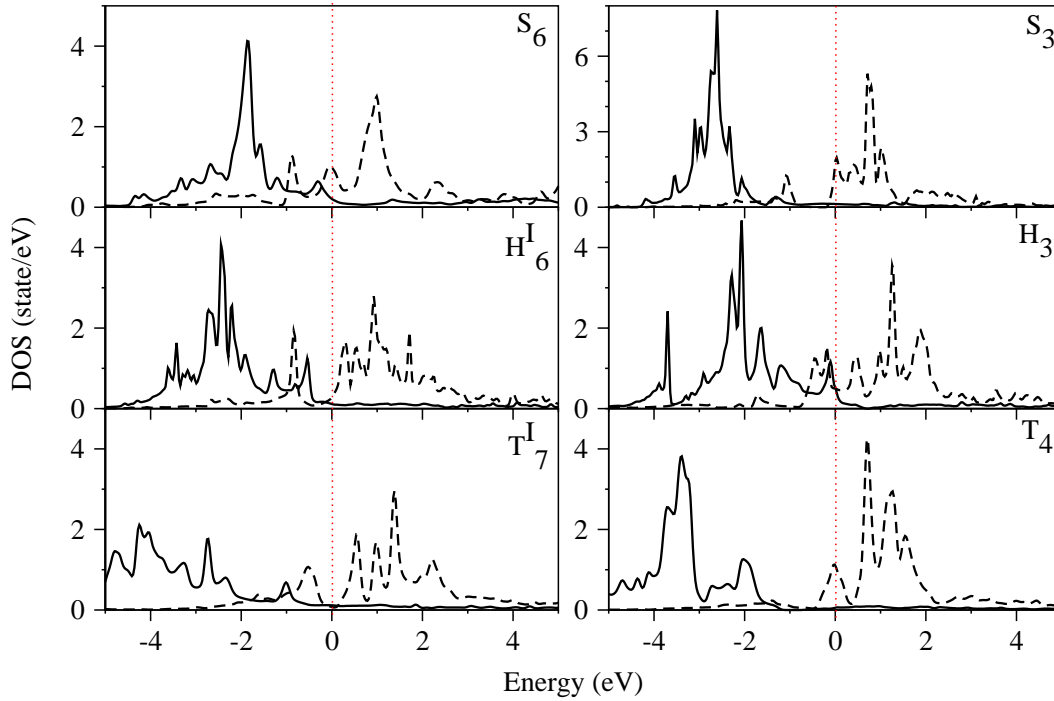creases the spin polarization [5] from 87% in T_4 to less than 20% in the T_7^I structure.

Fig. 7.4: Total density of states plot for Mn atom in S_6, S_3, H_3, H_6^I, T_4 and T_7^I configurations. The solid (dashed) lines indicate the projection of the spin up(down) wave function onto the d orbitals of manganese.

The presence of the Si-capping layer causes an energy gain in all configurations. We present a physical picture from analysis DOS plot which may leads to the stability these structures with Si-capping layer. In the structures with Si-capping layer (i.e. S_6, H_6^I and T_7^I) the Fermi level in DOS plot moves forwards in the energy range, which causes an energy gain is obtained by transferring some electrons from the unoccupied state above the Fermi level to the occupied states below the Fermi level in both spin channels. Therefore, structures with a Si-capping layer are more favorable than structures with a Mn-over layer.

For the substitutional site, the spin polarization at the Fermi level for a Si-capping layer structure is lower compared to the Mn-overlayer configuration by almost 20%, while the Si-capping layer increases the spin polarization for the Mn interstitial site. A comparison of the DOS plots for the low coverage of Mn/Si(001) and Mn/Si(111) shows that the exchange splitting of Mn-d orbitals in these structures is as large as the exchange splitting in a Mn-overlayer on Si(001), which is about 3-4 eV.

---

[5] Spin polarization is defined as: $\frac{\text{density of state(up)} - \text{density of state(dn)}}{\text{density of state(up)} + \text{density of state(dn)}}$

7.3   Morphology of Epitaxial Film on Si(111)

As discussed in Chap. 3, the cesium chloride (B2) and the nickel arsenide (AsNi) structures of Mn-mono-silicide do not exist as a bulk phase but there is a possibility that they could be grown epitaxially on a Si substrate [76]. The structure of these films is shown in Fig. 7.5. These structures are the two compatible epitaxial structures of Mn-mono silicide with the Si(111) substrate, having a small lattice mismatch of +2% for B2 and +7% for AsNi. In continuation of the topic of film growth on a Si substrate, the structural stability and magnetic properties of such films will be discussed in the following.

<center>(a)   (b)   (c)</center>
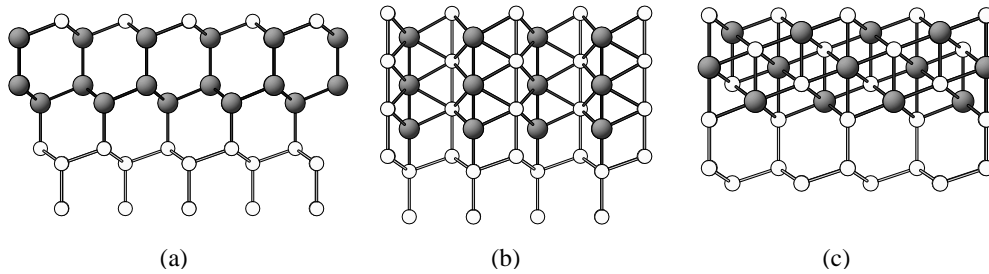
Fig. 7.5: The structures of a pure Mn film (a), a Mn-mono silicide with nickel arsenide structure (b) and a cesium chloride structure (c) are compared.

The formation energy and magnetic moments of the B2 and the AsNi structures for a coverage of $\theta = 1.5\,\mathrm{ML}$ are compared to the pure Mn film in Tab. 7.2. Following the results for Si(001), according to which the Si-capping layer increases the stability of a film, a Si capping layer is considered in all film calculations.

The film with B2 structure is more stable than with AsNi structure by $1.3\,\mathrm{eV}/(1 \times 1)$ cell. The formation energy of the film is calculated for equilibrium with bulk Mn and Si. Similar to the Mn/Si(001), the pure Mn-film is unfavorable, with a formation energy of more than $4\,\mathrm{eV}/(1 \times 1)$ cell higher than for a film with a B2 structure.

Due to the surface and the distortion of the film from and ideal cubic B2 structure, a considerable magnetic moment ($0.7\,\mu_\mathrm{B}$) is found for the Mn atom in the central layer. The vertical distance between layers is about 0.84 Å which is larger than for the bulk phase of B2 by maximum 5% . Mn in the surface and interface layer makes seven bonds with Si atoms at distances of 2.38-2.5 Å , while Mn in central layer has eight bonds to Si atoms.

The magnetic moments of Mn in the central layer of the AsNi structure is larger than its bulk value by $1.2\,\mu_\mathrm{B}$, which is due to the distortion of the structure compared to its bulk phase. The bonds between the Si-substrate and Mn-interface layer

Table 7.2: Formation energy, magnetic moment and spin polarization of different epitaxial structures of Mn-mono silicide on Si(111) at 1.5 ML coverage.

Structure	Formation energy eV/cell	Interface magnetic moment μ_B/layer	Surface magnetic moment μ_B/layer	Central layer magnetic moment μ_B/layer
Pure Mn	5.1	2.6	3.8	3.8
AsNi	2.03	2.4	2.7	2.7
CsCl(B2)	0.73	1.5	1.9	0.7

are slightly shorter than Si and Mn bonds at the central layers, which leads to smaller magnetic moment for the Mn at the interface.

The ferromagnetic coupling is found to be the most favorable magnetic struture for all films. The magnetic moment at the interface and surface are given in Tab. 7.2. The interface spin polarization at the Fermi level is 4%, 37% and 59% for pure Mn, AsNi and B2 structure films, respectively. Si layers between Mn layers have antiferromagnetic coupling with Mn atoms with small magnetic moment of $\sim$ –0.2 (–0.05) μ_B for AsNi (B2) structures.

In the following the stability and the magnetic structure of 3 ML of the B2 structure film on Si(111) will be compared to the similar film on the Si(001) surface

7.4   Comparison of B2 Structure of MnSi Film on Si(001) and Si(111)

The cutting of a B2 structure in the (111) direction is compatible with the Si(111) surface and can be suitably matched to it. In this structure Mn and Si layers of the film have the same atomic density as the substrate, therefore the thickness of such a film will be larger than for a film of B2(001)/Si(001) at the same coverage, Fig. 7.6.

The thermodynamic stability of a film with B2 structure on Si(111) is higher than on Si(001) by 0.12 eV/Mn atom. In addition to the B2 structure, the formation energy of a film with Mn_3Si structure is calculated. This structure contains three subsequent Mn-layers which are separated by one Si layer, see Fig. 7.6-c. The Mn_3Si structure on Si(111) is less stable than the B2 structure on the same surface by almost 0.14 eV/Mn atom. The magnetic moment of Mn at the surface and the interface is about 1.5 and 1.1 μ_B, respectively. The magnetic moment of Si in the central layer is almost zero but in the surface and interface a small negative magnetic moment of –0.06 and –0.01 on Si atoms appears. We discard this structure because of its higher

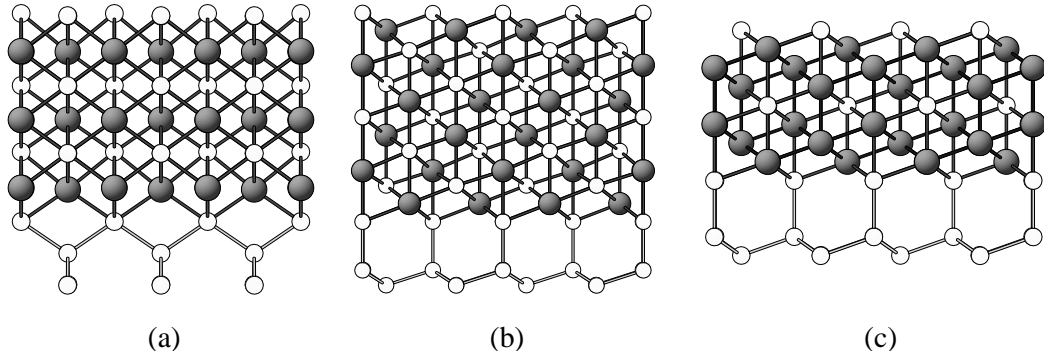(a)   (b)   (c)

Fig. 7.6: B2 structure on Si(001) substrate (a) and Si(111) surface (b) and the film with Mn$_3$Si structure on Si(111) (c) at coverage of 3 ML.

formation energy and continue with films with B2 structure.

The magnetic moments of Mn atoms at surface and interface are +1.8 μ_{B} and –2.0 μ_{B}. The average magnetic moment at central layers is about –0.5 μ_{B}. It was found on B2/Si(001) that, the spin magnetic moment of the central Mn layer almost vanishes (–0.15 μ_{B}),while for B2/Si(111) surface the central layer and also the surface and interface Mn atoms have higher magnetic moments than in case of the Si(001) substrate.

With increasing Mn coverage the distances between Mn-layers decrease slightly which results in a decreasing magnetic moment in the central layer.

The interlayer distances between Mn and Si layers are smaller for the inner layers compared to the outer layers.

Moreover, the magnetic state with interlayer AFM and FM coupling between the interface and surface Mn layers are calculated. There are several similarities between B2(001)/Si(001) and B2(111)/Si(111):

The spin magnetic moment of the central Mn layer is small, while the surface and interface Mn layers are magnetically active with the spin moment of -2.0 (1.8) μ_{B} for the interface (surface) layer Mn. The film formation of Mn-Si is more stable on the Si(111) compared to the Si(001) substrate.
This interlayer AFM structure is the magnetic ground state and has lower formation energy, $E_{\mathrm{form}} = -2.38 \, \mathrm{eV}/(1 \times 1)$ cell, than FM order by 18 meV/Mn.
The magnetic moments in the central layers starting from the interface and going towards the surface are -0.75 , -0.46 , -0.24 and +0.17 μ_{B} ,respectively (cf. Fig. 7.6). The central layer closest to the surface is magnetically almost inactive. The same argument as used in the case of the B2 film growth on a Si(001) substrate is valid here,

namely that a short Mn-Si bond length in the middle layer causes a strong covalent bond between Mn and Si, which reduces the already small magnetic moment of the central layer. Aditionally, the magnetic moment changes gradually over all these six layers from pointing downward in the interface to pointing upward at the surface.
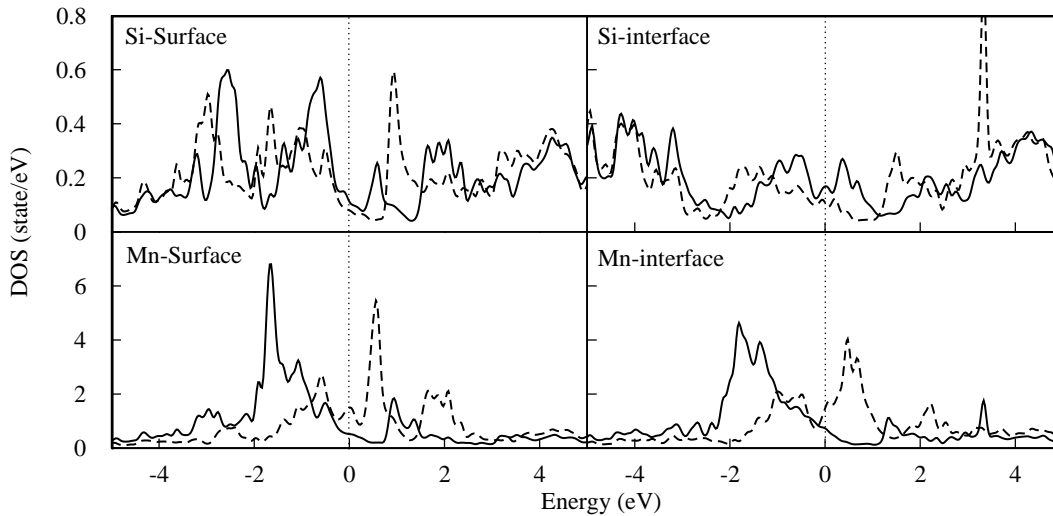

Fig. 7.7: DOS plot for the B2(111) structure on the Si(111) substrate at 3 ML coverage for Mn and Si atoms at interface and surface layer. Solid lines represent majority and dashed lines indicate minority spin channel, the dotted line shows the Fermi level.

The formation of a B2 structure film on Si(111), besides exhibiting a higher stability compared to the Si(001) case, also shows a high spin polarization of 33% and 49% at the interface and at the surface. This makes the growth of this structure on Si(111) more interesting than on Si(001).

Fig. 7.7 shows a DOS plot for B2(111)/Si(111). Clearly visible is the well defined peak for the majority spin DOS of Mn in the interface and surface layers and the Fermi level at the falling shoulder of the peak.

The thermodynamic stability of films with B2 structure on Si(111) and Si(001) as a function of coverage is shown in Fig. 7.8.

Here the formation energy of B2 film from 1-3 ML coverage in both Si surfaces are compared, red lines are B2(001)/Si(001) and black lines are B2(111)/Si(111). The dashed line which is considered as a zero reference is the surface energy of the bare surface. The formation energy of every structure consider in the case where it is in equilibrium with the bulk B20 structure of Mn-mono-silicide (circles), bulk B2 structure (triangles) and bulk Mn (squares) as reservoir.

According to this plot, the energy of film formation of B2 on Si(111) is smaller than on Si(001) in all coverages. The formation energy of the B2 film on both substrates is almost linear as a function of coverage.
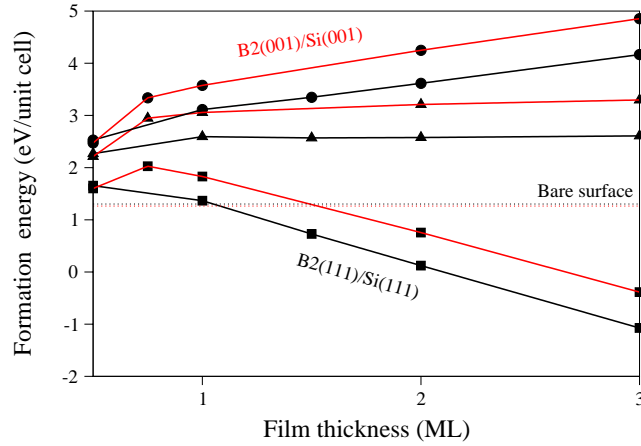

Fig. 7.8: Formation energy of film for B2 structure of Mn-mono-silicide on Si(001)(red lines) and Si(111)(black lines) substrates as a function of film thickness. Film formation is in equilibrium with bulk B20 structure of Mn-mono-silicide (circle signs), B2 structure of Mn-mono-silicide (triangle signs) and Mn (square signs). Surface energy of bare surface (dashed line) is considered as zero point.

As discussed before, the tendency of B2/Si(001) film to transform to three-dimensional islands and the bare surface for low coverage (≤ 2) makes formation of islands on this surface easier than on the Si(111) surface. However, on the other hand B2/Si(111) film formation energy is always decreasing with increasing the film thickness.

This comparison between these surfaces can be formulated as below:

$$\Delta E = \frac{1}{2}(\gamma_1 + \gamma_3) - \gamma_2$$

$$= \frac{(\gamma_3 - 2\gamma_2 + \gamma_1)}{2} \approx \frac{d^2\gamma}{d\theta^2} \tag{7.1}$$

Here, γ_i is the formation energy per area at ith ML coverage, and θ is the coverage. A positive value of ΔE, which is the second derivative of the formation energy with respect to coverage, corresponds to the positive curveture of the curve. This means formation of a homogenous 2 ML film is stable againt decomposition to islands. Therefore there is a barrier against surface roughness and formation of islands.

For a negative value of ΔE, the formation of a rough surface and areas with different film thicknesses are more favorable than a uniform film.

The formation energy of 2 ML is -0.51 eV/(1×1) cell which is higher than half of the sum of 1 ML and 3 ML by 0.03 eV/(1×1) cell. While in Si(111) formation of a uniform film with 2 ML coverage is more stable than 3 and 1 ML by 0.02 eV/(1×1) cell. Therefore one can conclude that from the thermodynamic point of view the formation of islands on Si(001) is easier and faster than on Si(111).

7.5   MnSi Surfaces

The low index Si(001) and Si(111) surfaces were studied in detail in Chap. 4. Here, the surface of MnSi in the B20(111) and B2(001) and (111) structures will be discussed.

- **B20(111) surface** The (111) surface of MnSi in the B20 structure has a in-plane hexagonal cell and four different surface terminations. The surfaces of the non-reconstructed (1×1) bulk-termination are considered in this work. These four terminations are the surface with Si-dense layer, Si-sparse layer, Mn-dense layer and Mn-sparse layer terminations, (cf. Fig. 7.5). The periodicity in z direction is 12 layers, therefore the slab contains 12 layers of Mn and Si atoms. Since there is no inversion symmetry in the slab, there are two different surfaces, (111) and ($\bar{1}\bar{1}\bar{1}$), in both sides of the slab.
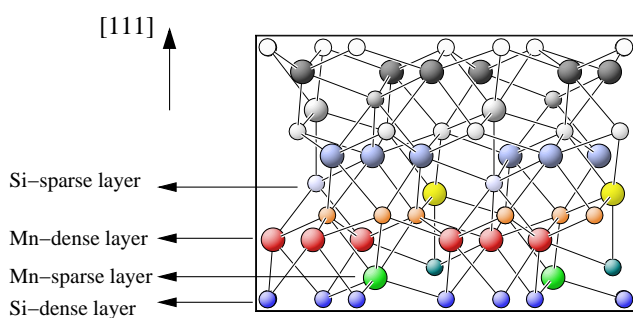

Fig. 7.9: Structure of four possible terminations of MnSi(111) in the B20 structure.

In these surfaces the top-most layer atomic configurations are exactly the same but the sub-surface layers are different. For example in Fig. 7.5, the top-most and the lowest layer of the slab are Si-dense layers but one of this surface connects to a Mn-dense layer below while below the other is a Mn-dilute layer. It is assumed that the surface energy of (111) and ($\bar{1}\bar{1}\bar{1}$) surfaces of the same type is very similar.

Since there are four (1×1) terminations, one needs to calculate the Gibbs free energy of each to find which one is the lowest-energy surface structure.

K. Reuter and M. Scheffler have described the formalism which combines thermo-dynamics and DFT total-energy calculations in order to determine the stable surface termination of compounds [163]. The most stable surface termination is the

one that has lowest surface energy, defined as:

$$\gamma(T,p) = \frac{1}{A}(G(T,p) - \sum_i N_i\mu_i(T,p))$$ (7.2)

Here γ is the surface energy, G is the Gibbs free energy of the slab, N_i and μ_i are the number and chemical potential of the ith of the constituent parts of the compound. The calculated surface energies of the four possible terminations of MnSi(111) in the B20 structure as a function of chemical potential of Mn are shown in Fig. 7.10. In order to calculate the surface energies, the bulk B20 crystal structure is considered as reservoir.
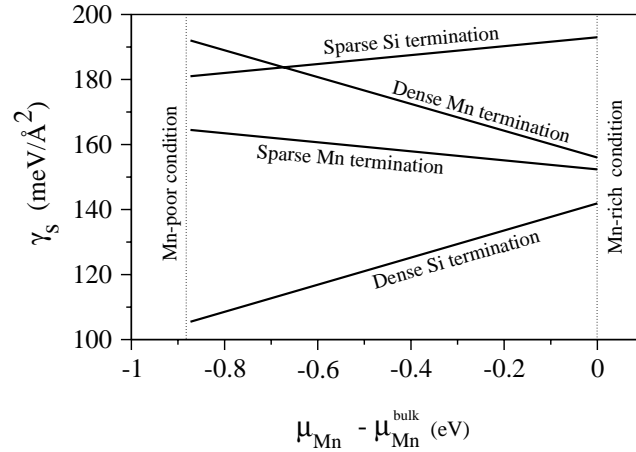

Fig. 7.10: Surface energy of the four terminations of MnSi(111) as a function of the chemical potential of Mn. The dotted vertical lines indicate the limit of the Mn chemical potential for Mn-rich and -poor conditions.

According to the phase diagram of the B20 structure, the dense-Si termination is the most stable termination over the whole Mn chemical potential range (see Fig. 7.10). The surface energy of B20 structure is about $62\,\text{meV}/\text{Å}^2$ (with respect to B2 crystal structure). The chemical potential of Mn in the Mn-poor limit corresponds to $\mu_{\text{Mn}} = \mu_{\text{MnSi}} - \mu_{\text{Si}}$ and the high limit of μ_{Mn} is taken as zero reference, and corresponds to the formation energy of bulk Mn. The lines belong to the Si (Mn) terminations and have positive (negative) slope, which indicates that the surface in Mn poor- (rich-) condition or equivalently in Si rich- (poor-) condition has more (less) stability.

Due to the increasing number of bonds, the magnetic moment of a Mn-dilute layer decreases from $2.8\,\mu_{\text{B}}$ to about $1\,\mu_{\text{B}}$ for a Mn-dense layer. The Mn atoms induce a small magnetic moment ($\sim$-0.05) in the topmost layer of Si atoms which have AFM coupling with the Mn atoms beneath.
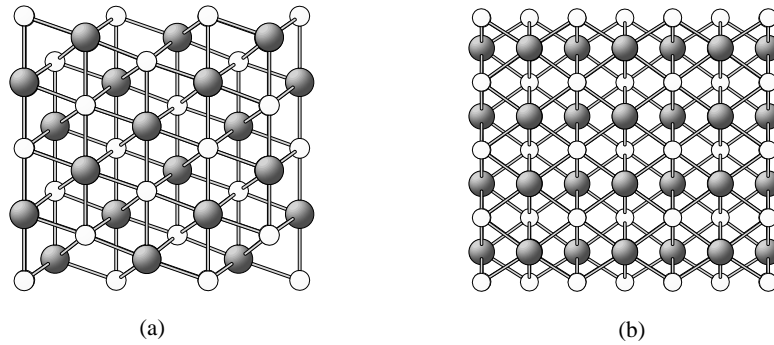
Fig. 7.11: Side view of the Si-termination of MnSi in B2 structure for a (111) surface (a) and a (001) surface (b). Small white (big black) circles are Si (Mn) atoms.

- **B2 structure** The (111) and (001) surface planes of the B2 structure of MnSi with Si-termination are show in Fig. 7.5-a,b. The surface energy of B2(111)(1×1) is lower than that of B2(001) by $18.5 \, \text{meV}/\text{Å}^2$. The surface energy of B2(111) is about $39 \, \text{meV}/\text{Å}^2$ more than surface energy of the B20 structure. The surface energies of all surfaces are summarized in Tab. 7.3 in Sec. 7.7. The B2(001) slab contains alternating planes of dense Mn and Si atoms with a lateral distance of $2 \, \text{Å}$ and vertical distances of 1.2-$1.4 \, \text{Å}$. In contrast, for the B2(111) surface the intralayer atomic distance is $4 \, \text{Å}$ with the vertical interlayer distances of 0.8-$0.9 \, \text{Å}$ between Mn and Si.

Mn in both slabs with the B2 structure has eight bonds in the central layers, which is consistent with a small magnetic moment of 0.2 and 0.5 μ_B for Mn in the (001) and the (111) slab, respectively. Due to the lack of a bond of Mn at the (111) surface , the magnetic moments of Mn atoms at the surface increase to 1.8 μ_B, while in the (001) surface the Mn atom still has eight bonds and a small magnetic moments of 0.2 μ_B.

7.6 MnSi Films with B20 Structure

In continuation of the work on film morphology, we study the stability of the natural structure of MnSi (B20). This structure is considered at low coverage (up to $4/3 \, \text{ML}$). In the B20 structure $0.5 \, \text{ML}$ coverage corresponds to a $\sqrt{3} \times \sqrt{3}$ cell containing three Mn atoms. The structure for $\theta = 2/3 \, \text{ML}$ in top view and side view is shown in fig. 7.12.

The formation energy of the films with B20 structure is always less than those with the B2 structure over all coverages. The formation energy of such films on Si(111) is compared with the corresponding formation energy of the films with the B2 struc-
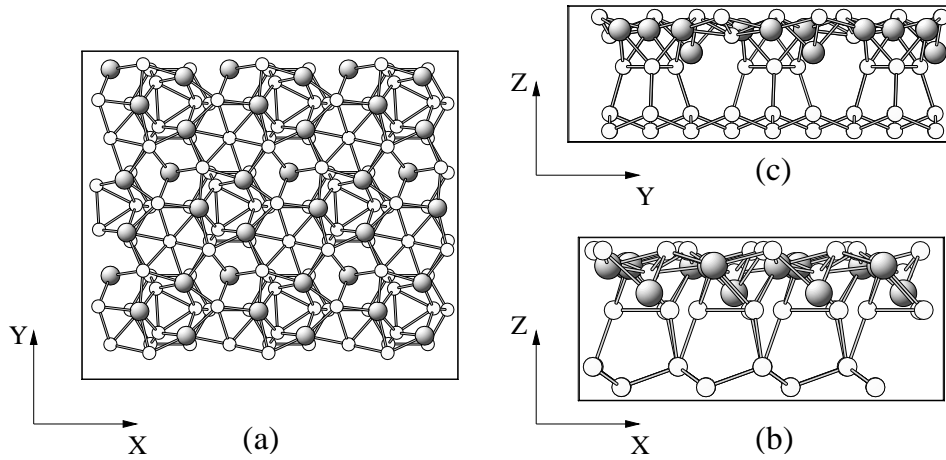
Fig. 7.12: Top view (a) and side view (b-c) of B20 of Mn-mono-silicide structure at coverage of $\theta = 2/3\,\mathrm{ML}$.

ture for coverages from 0.5-1.5 ML in Fig. 7.13.

Similar to previous consideration, the stability of these films is calculated with respect to the reservoir of either bulk Mn (squares), or bulk MnSi in the B2 structure (triangles) or in the B20 structure (circles) of Mn-mono-silicide. The dashed lines represent B2/Si(111) and the solid lines correspond to B20/Si(111).

The energy of film formation of B20/Si(111) with respect to bulk B20 is almost constant, about 1.1 eV/(1×1) unit cell, while its formation energy decreases with respect to bulk Mn and the B2 structure of Mn-monosilicide. However, the formation energy of the B20 film is still higher than the energy of the bare Si(111) surface.

The average magnetic moments at $\theta = 8/6\,\mathrm{ML}$ coverage is about 2.3, 0.9 and 3.4 μ_{B} at the surface, the central and the interface layers which are higher than the magnetic moment of a film with the B2 structure at similar coverage. The parallel spin moment coupling is considered for Mn atoms in-plane as well as between layers. With increasing of the film thickness the magnetic moments at surface and interface increase. According to the DOS plot, the film with B20 structure is a metallic film with the interfacial and surface spin polarization of more than 50%.

Finally, we come to the conclusion that thermodynamically formation of a homogenous wetting Mn-mono silicide film on the Si substrate is metastable and formation of islands of metallic Mn-mono-silicide with $(\sqrt{3} \times \sqrt{3})$R30° cell is favorable. Such an island has considerable magnetization and spin polarization at interface and surface.
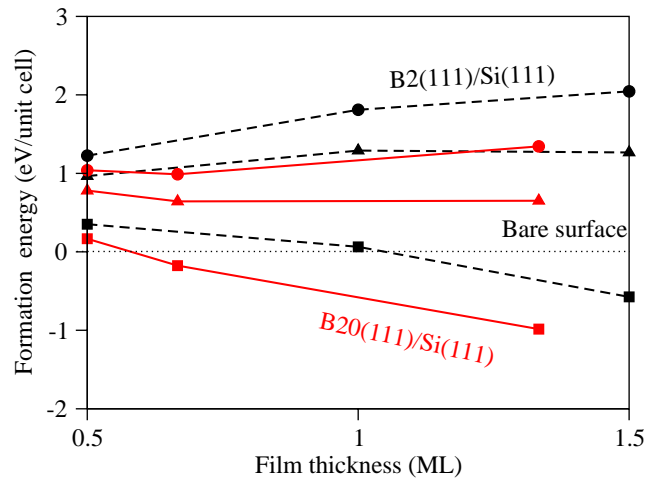
Fig. 7.13: Formation energy of ultrathin film for B2 (black lines) and B20 (red lines) structure of Mn-mono-silicide on Si(111) substrates as a function of film thickness. The energy of film formation is calculated by assuming equilibrium either with the B20 bulk structure of Mn-mono-silicide (circles), or the B2 structure of Mn-mono-silicide (triangles) or Mn bulk (squares). The surface energy of the bare Si(111)(1×1) surface (dotted line) is considered as zero point.

7.7 Growth Mode of Mn-Monosilicide in B2 Structures on Si Substrates

Studies of the surface morphology of epitaxial growth attract attention since their development help to explain the stability of nanostructures, islands or film formation on the surface.

Thin film growth usually falls into one of three broad categories: Frank van der Merwe (layer by layer growth), Volmer-Weber (island formation growth), and Stranski-Krastanov (layer growth followed by island formation), Fig. 7.7 [143]. This scheme of classification is well understood and works for the vast majority of systems investigated.

Quantitatively, each system adopts a unique growth mode depending on the relative magnitude of its surface and interface energies.

In a simple description, the growth mode can be attributed to the lattice match between the substrate and the film. Existence of a lattice mismatch creates strain in the film which leads to formation of three-dimensional (3D) islands (either Volmer-Weber or Stranski-Krastanov growth mode). Thermodynamically, this growth regime is more favorable than formation of a homogenous film. The small lattice mismatch between substrate and film causes first formation of a wetting layer and subsequently formation of islands on this wetting layer (Stranski-Krastanov growth

mode). On the other hand, in the large lattice mismatch regime, the growth process will end up in the Volmer-Weber growth mode in which the islands form on the bare surface.

$$\Delta\gamma = \gamma_{\text{film}} - \gamma_{\text{substrate}} + \gamma_{\text{interface}} \tag{7.3}$$

$$\begin{cases} \gamma_{\text{substrate}} > \gamma_{\text{film}} + \gamma_{\text{interface}} & \text{Frank} - \text{van der Merwe} \\[2ex] \gamma_{\text{substrate}} < \gamma_{\text{film}} + \gamma_{\text{interface}} & \text{Volmer} - \text{Weber / Stranski} - \text{Krastanov} \end{cases} \tag{7.4}$$

here, γ_{subs}, γ_{film} and γ_{inter} are the surface energy of the surface, the formation energy of a film and the interface energy per area.
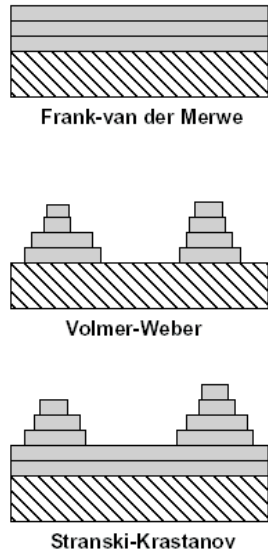

Fig. 7.14: Schematic illustration of different growth modes of heteroepitaxial growth.

If the energy of the film and of the interface per area is lower than the surface energy of the substrate, a layer-by-layer growth mode will be preferred, while a lower surface energy of the substrate would lead to formation of islands.

As it was discussed in Sec. 7.4 in the competition between island and film formation, it is more favorable at low coverage that islands form instead of a uniform epitaxial film on Si(001). It can be explained by the energy gain due to relaxation in an island which overcompensates the energy cost of increasing the surface energy by the side facets of the island [164]. However, since formation of island's facets costs energy, therefore island formation is not instantaneous and it will form only at certain coverage of adsorbate and island density. In order to study this surface roughness one needs to find the conditions for nucleation of islands and the optimum island size for a given coverage and island density. In the following part, the critical size for island formation will be calculated.

7.7.1   Formation of MnSi Nano-Structures on Si Substrates

The formation and stability of island and film were calculated for InAs/GaAs by Wang *et al.* [164]. They calculated the energy gain for an island assuming that islands form with a identical shape and size, in equilibrium with the wetting layer.

Since the lattice mismatch between the Si substrate and the B2 structure of MnSi is small (less than 2%), the formalism which is used in this work is a bit different. Here, the elastic energy density which is introduced by strain is neglected. We consider a pyramidal-shaped island of MnSi with a square or triangle base (with a base length of a) on the substrate.

The real island shapes are more complex, having complicated facets. However, already such a simple island shape allows a preliminary estimate of basic features of the island formation. It is supposed that the island which forms on Si(001) has four (111) facets and the tetrahedral island on Si(111) has three (001) facets, cf. Fig. 7.15.
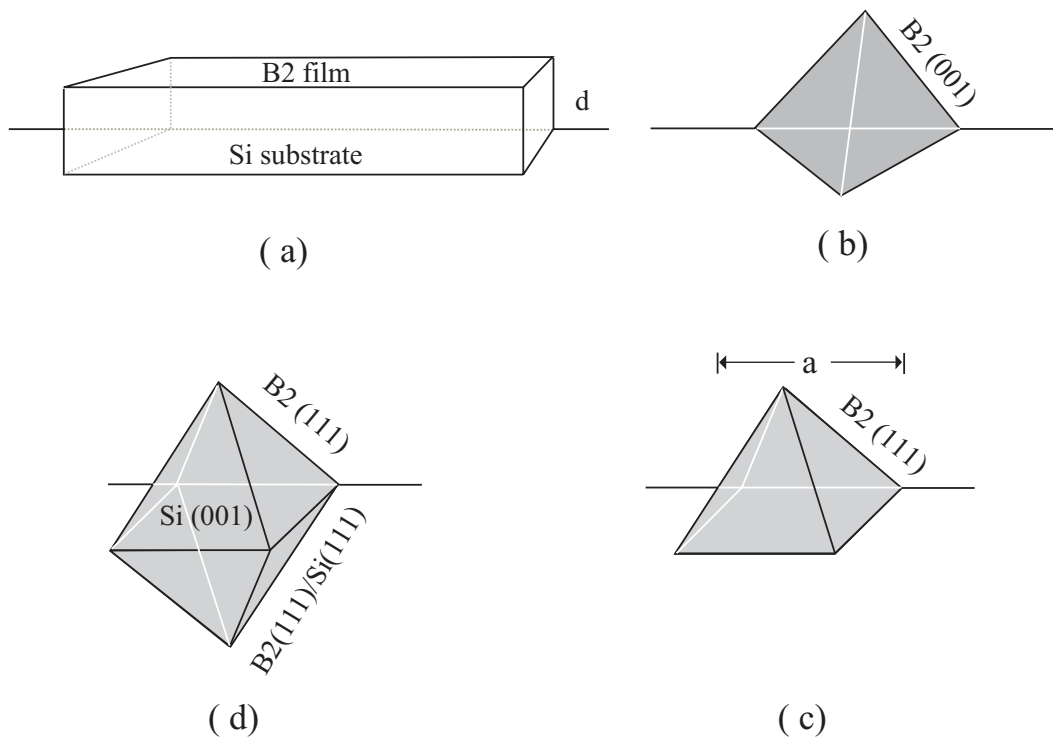
Fig. 7.15: Schematic illustration of film formation with thickness d (a) and island formation with island base length a. On the Si(111) substrate, the tetrahedral-shaped-islands with B2(001) facets (b) will form and on the Si(001) substrate, the pyramid islands with B2(111) facets (c). The iceberg island (d) with B2 structure can form on both Si substrates.

Figure 7.15 schematically illustrates the island formation on the substrate surface. d is the thickness of the film.

The equilibrium condition between film and island can be described as:

$$A_{\text{film}}\gamma_{\text{film}} = (A_{\text{film}} - A_{\text{interface}})\gamma_{\text{substrate}} + A_{\text{interface}}\gamma_{\text{interface}} + N \times A_{\text{facet}}\gamma_{\text{island}} \quad (7.5)$$

where $\gamma_{\text{film}} = \gamma_{\text{surface}} + \gamma_{\text{interface}}$ is the formation energy of the wetting layer per unit area. It consists of the surface energy of the wetting layer (γ_{surface}) and the interface energy per unit area ($\gamma_{\text{interface}}$). $\gamma_{\text{substrate}}$ and γ_{island} are the surface energy of the bare substrate and the surface energy of the facet of an island. A_{film} and A_{facet} are the area of the wetting film and the facets, and N is the number of facets.

In the present work all surface energies are evaluated with respect to being in equilibrium with a bulk of MnSi in a $B2$ (CsCl) structure (i.e., $\mu_{\text{Mn}} = \mu_{\text{MnSi}}^{\text{bulk}} - \mu_{\text{Si}}^{\text{bulk}}$). From mass conservation it can be deduced, that the volume of an island V is given by:

$$\frac{V}{v_{\text{atom}}} = \frac{1}{6}\, a^3\, \frac{\tan\alpha}{v_{\text{atom}}^{\text{island}}} = A_{\text{film}} \times \frac{d}{v_{\text{atom}}^{\text{film}}} \quad (7.6)$$

where α is the angle between the island facets and the substrate (cf. Fig. 7.15) and d is the thickness of the film [164]. $v_{\text{atom}}^{\text{island}}$ and $v_{\text{atom}}^{\text{film}}$ are atomic volume of MnSi in crystal structures of islands and film, respectively. Since crystal structure and bond lengths in B2 and B20 structures are different, therefore their islands have not the same volume. Thus $A_{\text{film}} = \frac{V}{d} \cdot v_{\text{atom}}^{\text{film}}/v_{\text{atom}}^{\text{island}}$. In this work, the film has only B2 structure and the islands have either B2 or B20 structures. According to the calculation in the Chap. 3 the volume of a Mn atom in B20 and B2 crystal structures is 23.04 and 21.84 Å^3, respectively.

Since the formation enthalpy of the B20 structure is lower than that of the B2 structure by ~ 0.26 eV/formula unit, one should take into the account an extra term ($\epsilon = \Delta H \cdot V/v_{\text{atom}}^{\text{B20}}$) to eq. 7.5 for the B20 islands formation. The energy release to form a B20 island from a film with B2 structure is about 0.011 eV/Å^3.

The total energy difference between film and island formation per unit volume of a single island can be expressed as:

$$\Delta E/V = \frac{(\gamma_{\text{substrate}} - \gamma_{\text{film}})}{d}(v_{\text{atom}}^{\text{film}}/v_{\text{atom}}^{\text{island}})$$
$$+ [A_{\text{interface}}\,(\gamma_{\text{interface}} - \gamma_{\text{substrate}}) + N \times A_{\text{facet}}\,\gamma_{\text{island}}]/V - \epsilon \quad (7.7)$$

A positive value of ΔE indicates that film formation with B2 structure of Mn mono-

silicide is more stable than island nucleation, while a negative value favors the stability of islands.

The surface energy for a non-reconstructed (1×1) ideal surface termination at low index silicon surfaces as well as for MnSi surfaces in the B2 and B20 structures are given in Tab. 7.3. For Si surfaces the surface energy is compared to the surface energy calculated by Stekolnikov and Bechstedt (S-B) [6].

In order to a calculate the surface energy, bulk silicon and MnSi in B2 structure are considered as reservoirs. The surface energy of the Si(111) surface is less than that of the Si(001) but the B20(111) surface is the most stable surface. Therefore, formation of a wetting layer with the natural MnSi film should be more stable on Si(111) than an epitaxial film with B2 structure.

Table 7.3: Surface energy, γ_{surface} (meV/Å^2) of non-reconstructed Si and MnSi surfaces. Bulk MnSi in the B2 structure is considered as a reservoir for the chemical potential of Mn. The calculated surface energies from Stekolnikov and Bechstedt (S-B) [6] are for a Si(001)c(4×2) and a Si(111)(7×7) reconstruction.

Surface	Present work GGA	Ref.	S-B work LDA
Si(001)(1×1)	136	Sec. 4.2.1	149
Si(001)(2×2)	84	Sec. 4.2.3	88
Si(111)(1×1)	100	Sec. 4.3	109
Si(111)(7×7)	81*	—	85
MnSi(B2)(001)	118	Sec. 7.5	—
MnSi(B2)(111)	101	Sec. 7.5	—
MnSi(B20)(111)	62	Sec. 7.5	—

(*) The surface energy of the reconstructed Si(111)(7×7) is extrapolated from the LDA calculation of S-B work.

In Tab. 7.4 the film thickness (d), facet area (A_{facet}), volume of island (V_{island}), energy of film formation (γ_{film}) and interface energy ($\gamma_{\text{interface}}$) per area for MnSi in B2 and B20 structure in Si(001) and Si(111) are given. The films thickness in Tab. 7.4 corresponds to 3 ML Mn coverage. The surface energies of Si(001) and Si(111) are compared to Stekolnikov and Bechstedt (S-B) work which was done using the LDA functional [6].

The film growth on Si(111) is more favorable than an Si(001) and formation of the B20 structure is easier than of the B2 structure. The interface energy of the B20 structure is the lowest value. However, the interface energy in Si(001) and Si(111) depends on the kind of island which forms on each substrate (cf. Tab. 7.5).

Table 7.4: Film thickness, d, facet area A_{facet} energy of film formation per area, γ_{film}, and surface energy of the bare surface. For Si, the reconstructed surfaces are considered while for MnSi, the non-reconstructed surface is considered.

Film	d Å	A_{facet} Å^2	γ_{film} meV/Å^2	$\gamma_{\text{substrate}}$ meV/Å^2	Ref.
B2(001)/Si(001)	7.51	$(\sqrt{3}/4)a^2$	219	88	Sec. 6.4
B2(111)/Si(111)	8.87	$(1/4)a^2$	200	85	Sec. 7.4
B20(111)/Si(111)	8.00	$(1/4)a^2$	148	85	Sec. 7.6

There are three kinds of islands that can form on Si(001), the pyramid shape with 4 facets with B2 structure, the iceberg island with B2 structure and the iceberg island with B20 structure. In the pyramid island there is an interface between the B2(001) film and the bare surface of Si(001). In the iceberg island there are four interfacial facets which have B2 (B20) structure on Si(111).

Because the B20 structure is not compatible with Si(001), therefore the energy of such interface is not calculated and the formation of an iceberg island with B20 structure on Si(111) is discarded.

The interface of a pyramid island on Si(001) is a square with a^2 and iceberg islands have 4 facets with $(\sqrt{3}/4)\ a^2$ area of each facet. The interface of a pyramid island on Si(111) has a triangle base shape with $(\sqrt{3}/4)\ a^2$ area and the interface area of the iceberg island is three triangles.

The critical base lengths for nucleation of different kind of islands on both Si(001) and Si(111) are given in Tab. 7.5 for a given thickness of the film (which is mentioned above Tab. 7.4) .

As one can see from the values of the stable island size, formation of an iceberg island with B20 structure on Si(001) is faster than other kind of island on both surface orientations. On Si(001), islands form earlier than in Si(111), and the film on Si(111) is more stable than on Si(001). Additionally, the iceberg form of the island is more favorable than the pyramid shape and in Si(001) islands have B20 structure. The island size of the B20 structure on Si(001) with iceberg shape is only 15.0 Å which is almost 3 times the lattice constant of Mn-mono silicide in B20 crystal bulk[6]. Therefore this nano-structure on Si(001) can from rapidly, in contrast to formation of pyramid islands on Si(111), which should be rare, because the base length for island formation is about 30 times the lattice constant of Mn-mono silicide in the

---

[6]The lattice constant of B20 structure of Mn-mono silicide is 4.5 Å, see Sec. 3.4.1

Table 7.5: Area of interface and volume of islands, interface energy per area, $\gamma_{\text{interface}}$ and stable island size a_0 for island formation. Bulk MnSi in B2 structure is considered as reservoir for calculating the chemical potential of Mn.

Film		$A_{\text{interface}}$ Å^2	V_{island} Å^3	$\gamma_{\text{interface}}$ meV/Å^2	a_0 Å
B2(001)	Pyramid B2	a^2	$\frac{\sqrt{2}}{6} a^3$	101	52.0
on	Iceberg B2	$\sqrt{3}\, a^2$	$\frac{\sqrt{2}}{3} a^3$	99	28.0
Si(001)	Iceberg B20	$\sqrt{3}\, a^2$	$\frac{\sqrt{2}}{3} a^3$	86	15.0
B2(111)	Pyramid B2	$\frac{\sqrt{3}}{4} a^2$	$\frac{1}{12\sqrt{2}} a^3$	99	133.2
on Si(111)	Iceberg B2	$\frac{3}{4} a^2$	$\frac{1}{6\sqrt{2}} a^3$	101	71.3

B20 structure.

With island size larger than the stable value, a_0, ΔE has negative value which means that the growth of the islands become exothermic.

$\star\ \star\ \star\ \star$